NACA

RESEARCH MEMORANDUM

QUALITATIVE STUDY OF FLOW CHARACTERISTICS THROUGH

SINGLE-STAGE TURBINES AS MADE FROM

ROTOR-EXIT SURVEYS

By Robert Y. Wong, James W. Miser, and Warner L. Stewart

Lewis Flight Propulsion Laboratory
Cleveland, Ohio

CLASSIFICATION CHANGED

UNCLASSIFIED

To_____

By authority of____ YRN-123 ____ Date Dec. 13, 1957

AMT 1-20-58

NATIONAL ADVISORY COMMITTEE
FOR AERONAUTICS

WASHINGTON

March 2, 1956

3889

CI-1

NATIONAL ADVISORY COMMITTEE FOR AERONAUTICS

RESEARCH MEMORANDUM

QUALITATIVE STUDY OF FLOW CHARACTERISTICS THROUGH SINGLE-STAGE

TURBINES AS MADE FROM ROTOR-EXIT SURVEYS

By Robert Y. Wong, James W. Miser, and Warner L. Stewart

SUMMARY

In view of the complex nature of the flow through a single-stage turbine and its effects on rotor-exit survey results, a study of the survey results obtained from two transonic turbines was made in an effort to gain an insight into the physical aspect of the flow. Some of the major factors that influence the measured flow patterns were qualitatively isolated in order to facilitate the analysis. The two transonic turbines used as examples differed primarily in that one had a relatively high diffusion on the rotor suction surface, while the other had a relatively high diffusion on the rotor pressure surface.

The results indicate that the flow characteristics through a single-stage turbine can be deduced from rotor-exit surveys. Considerable circumferential variation existed in angular momentum at the rotor inlet, which is attributable to momentum variations in the regions of stator free-stream flow. Large radial variations in angular momentum and total-pressure loss were also found at the rotor exit.

The two turbines differed markedly in the radial variation in rotor total-pressure loss and rotor-outlet angular momentum because of two factors: (1) the blade surface upon which the high diffusion and therefore the high loss occurred, and (2) the subsequent secondary-flow path which the low-velocity fluids followed through the rotor.

Premature choking of the turbine rotor with high suction-surface diffusion was indicated by higher-than-design rotor-outlet angular momentum at design work output. A slight mismatch between stator and rotor throat areas of the high-pressure-surface-diffusion turbine was indicated by lower-than-design rotor-outlet angular momentum at design work output.

INTRODUCTION

The flow characteristics through a single-stage turbomachine may be thought of as a three-dimensional potential-flow field upon which are

superimposed other complicating effects. These other effects include viscous-flow losses due to the blades and wall surfaces of the machines and secondary flows that occur both within and downstream of each blade row. This complicated flow field results in certain flow patterns that may be measured by making detailed surveys immediately downstream of the machine.

In order to analyze and interpret the survey results obtained at the rotor exit, it is necessary to separate the various effects and evaluate their individual contribution to the over-all picture. A quantitative evaluation of this kind is made difficult by the effects of mixing. A qualitative evaluation of these rotor-exit surveys may be accomplished through the use of the measured flow conditions out of the stator and from consideration of certain limitations that are inherent in the survey instrumentation.

The flow characteristics through two single-stage transonic turbines are described herein. This description is based on results of rotor-exit surveys at approximately design-point operation reported in references 1 and 2. The distinguishing difference in the design characteristics is that the turbine in reference 1 was designed for a relatively high diffusion on the rotor blade suction surface while that of reference 2 was designed for a relatively high diffusion on the rotor blade pressure surface. The survey results of the two turbines demonstrate typical flow patterns that may be found immediately downstream of a single-stage turbine rotor. Some of the major factors that influence the indicated flow patterns are also discussed.

TURBINE DESIGN CHARACTERISTICS

The turbines used in this investigation were designed for identical rotor-inlet velocity diagrams. Thus, the design rotor tip speed and design weight flow were also identical. The rotor-exit velocity diagrams of the two rotors differed, resulting in slightly different levels of work output and different degrees of reaction across the rotor. The distinguishing difference, however, is that the turbine rotor of reference 1 was designed for a relatively high diffusion on the suction surface, while the rotor of reference 2 was designed for a relatively high diffusion on the pressure surface. The turbine with the high diffusion on the rotor suction surface is designated herein as turbine 1, and the turbine with the high diffusion on the rotor pressure surface is designated as turbine 2.

The mean-radius rotor blade profiles and design velocity distributions for both turbines are shown in figure 1. The blades were designed for a sharp leading edge and then rounded off to a minimum practical radius upon fabrication. The design surface velocity distributions indicate the amount of diffusion taken on each surface. Further, turbine

1 has a much higher diffusion on the suction surface than turbine 2. Thus, much larger losses on the suction surface of turbine 1 are anticipated. On the pressure surface, turbine 2 has a much higher diffusion than turbine 1, and much higher losses are anticipated on the pressure surface of turbine 2. The midchannel velocity distribution shows that the over-all rotor reaction of turbine 2 is greater than that of turbine 1.

The performance of these turbines has been investigated experimentally (refs. 1 and 2). The design-point efficiency is 0.813 and 0.869 for turbines 1 and 2, respectively.

BASIS FOR ANALYSIS

In order to gain an insight into the physical aspects of the flow as it passes through a single-stage turbine, it is necessary to separate qualitatively the major factors that influence the flow patterns measured at the rotor exit. This can be accomplished from consideration of the effect of time-response limitations of the survey instrumentation on the indicated flow patterns and by study of the stator-exit survey results.

Stator-exit survey results show that, in the regions of stator free-stream flow (region between the blade wakes and end-wall regions), the radial variation in total pressure is small. If these regions of flow can be identified downstream of the rotor, then any large radial variations in total pressure measured in these regions can be attributed to effects within the rotor. Any radial variation of total pressure in these regions, however, results from the combined effects of radial variations in rotor work output and rotor-induced losses. In order to obtain an indication as to the radial variation in rotor total-pressure loss, it is necessary to separate the two effects. They can be separated by computing a total-pressure-loss parameter L from the following equation:

$$L = 1 - \frac{P_o'}{P_i'} \left(\frac{T_i'}{T_o'}\right)^{\frac{\gamma}{\gamma-1}}$$

(Symbols are defined in appendix A.) This parameter represents an overall total-pressure loss which is the product of the stator and rotor relative total-pressure ratios. By using the local values of total temperature and total pressure, local values of turbine loss are obtained. Contours of total-pressure-loss parameter for both turbines are presented.

The regions of stator free-stream flow at the rotor exit can be identified in the following manner. In single-stage turbines, circumferential variations in total pressure (shown schematically in fig. 2)

are induced by both the stator and the rotor. The circumferential varia-
tions relative to the rotor move tangentially at the speed of the rotor.
As a result of the time-response limitations of the probe, the circum-
ferential variations relative to the rotor are time-averaged by the probe.
The circumferential variations induced by the stator, however, pass
through the rotor with turbulent mixing. Thus, as the probe is moved
circumferentially, a variation in probe reading may be recorded. This
variation must then originate from the stator, since all circumferential
variations relative to the rotor are averaged out. The regions of stator
free-stream flow downstream of the rotor can now be identified by assum-
ing that at a given radius the point of minimum total-pressure-loss pa-
rameter L corresponds to stator free-stream flow that is least affected
by mixing of the stator losses.

Using these concepts on the survey results of references 1 and 2
makes it possible to gain an insight into some of the major factors that
influence the measured flow patterns. These factors may then be identi-
fied as to their origin and possible explanations presented.

RESULTS AND DISCUSSION

Contours of over-all local adiabatic efficiency are presented in
figure 3 for both turbines. The contours of efficiency are based on
measurements of total pressure and total temperature taken from the tur-
bine inlet and from surveys taken at the turbine outlet. The survey
measurements were taken approximately 1/4 inch downstream of rotor exit,
by making circumferential traverses with a probe placed at various radial
stations. The survey covered a segment of annulus corresponding to ap-
proximately $1\frac{1}{4}$ stator pitch. These efficiency contours were previously
reported in references 1 and 2. Contours of measured total-temperature
drop and total-pressure drop are given in figures 4 and 5, respectively,
for both turbines.

Circumferential surveys of absolute rotor-exit flow angle at various
radial stations were also made. However, the variation in the flow angle
across the circumferential traverse was very small because of the effects
of mixing, which tends to smooth out the stator-induced variations, and
the effects of the probe, which time-averages any circumferential varia-
tion relative to the rotor. Thus, only the radial variation of the cir-
cumferentially averaged angle is presented in figure 6 for both turbines.
The negative values of rotor-exit angles mean that the absolute flow was
turned past the axial direction to the direction opposite that of rotor
rotation.

The efficiency contours in figure 3 indicate that a decrease in ef-
ficiency occurs in the tip region of turbine 1 and in the mean-radius

region of turbine 2. Circumferential variations in local efficiency can also be noted. In order to gain an insight into the physical aspects of the flow that are represented by the various regions of loss, the various survey plots will be considered in an effort to qualitatively separate some of the major effects.

Momentum Variation

Since at a given radius the total change in angular momentum is proportional to the total-temperature drop measured at that radius, the contours of total-temperature drop (fig. 4) are also contours of total change in angular momentum. In order to facilitate the analysis of these contours, it is expedient to separate the total change in angular momentum into plots of rotor-inlet and -outlet angular momentum. This can be accomplished by noting that any circumferential variations in angular momentum relative to the rotor cannot affect the reading of the probe because of limited time response. Thus, as the probe is moved circumferentially at a given radial station downstream of the rotor, only circumferential variation in rotor-inlet angular momentum can affect the total-temperature readings. As the probe is moved from one radial station to another, however, radial variations in rotor-outlet angular momentum can affect the probe reading. An approximation of the radial variation in rotor-outlet angular momentum can be obtained from measured values of total pressure, static pressure, total temperature, and absolute exit flow angle as described in appendix B.

The radial variation in rotor-exit angular momentum computed by this method is plotted in figure 7 in terms of an angular-momentum parameter, $\omega r V_{u,M}/gJc_p T_i'$. Included for comparison is the radial variation in the design values of rotor-exit angular momentum. Comparison of the design and measured rotor-outlet angular-momentum parameters for turbine 1 indicates that considerable negative exit angular momentum was required in order to obtain design work output. This means that the rotor was prematurely choked, which in turn resulted in reduced velocities and, therefore, reduced angular momentum out of the stator. Thus, in order to obtain design work, overexpansion of the flow out of the rotor was required, which resulted in negative angular momentum at rotor exit. Further inspection of the rotor-outlet angular-momentum curve for turbine 1 shows that a very large variation from hub to tip exists, the region near the tip having the largest negative angular momentum.

Comparison of the design and measured rotor-exit angular-momentum parameter for turbine 2 indicates that the measured angular momentum in general is a smaller negative value than design. This means that, in order to obtain design work, a higher-than-design angular momentum must have occurred at the rotor inlet. This could have occurred if there was

a slight mismatch between the rotor and stator throat areas such as to
cause a slight overexpansion in stator flow. Again, there is a large
variation in angular momentum from hub to tip, the region of largest
angular-momentum deficiency occurring in the region of the mean radius.
The hub and tip regions appear to operate very near design.

With the use of the curves of rotor-exit angular-momentum parameter
(fig. 7), the temperature-drop contours (fig. 4) were adjusted so that
the rotor-outlet angular momentum was removed. This was done by sub-
tracting the rotor-exit angular-momentum parameter at a given radius from
the measured temperature drop at every circumferential point at that
radius. The results of this adjustment are plotted in figure 8 for both
turbines. These contours approximate the angular-momentum variations
that enter the rotor. With the effects of the rotor removed, much more
uniform conditions exist in the region of stator free-stream flow down-
stream of the rotor. The region of stator free-stream flow is believed
to extend from the lower right corner toward the upper left corner of the
figure and in the regions of higher angular momentum. It is evident from
the angle of inclination of these patterns that the stator flow patterns
were considerably distorted in passing through the rotor.

A marked decrease in angular momentum is evident in the tip region
of turbine 1, indicating that flow is choked downstream of this region.
This choking results in a shift in the streamlines toward the hub in this
region, which in turn results in reduced velocities.

In addition to the radial variation in rotor-inlet angular momentum,
large circumferential variations are also noted (fig. 8). In order to
gain an insight into the cause of these variations, the pressure-drop,
efficiency, and temperature-drop contours were compared. In general, the
regions of high temperature drop or high change in angular momentum across
the rotor (fig. 4) correspond to the regions of lower efficiency (fig. 3)
and high total-pressure drop (fig. 5). In the regions of low temperature
drop or low change in angular momentum across the rotor, a higher effi-
ciency was noted with a lower total-pressure drop. The peak efficiency
regions occurred between the regions of high and low temperature drop.

In the stator wake regions the velocity is lower than that of the
free stream. Thus, if the wake regions pass through the rotor intact, a
region of low change in angular momentum or low temperature drop would
correspond to a region of low local efficiency. A low local efficiency
would be expected because of (1) the total-pressure loss in the stator
wakes and (2) high negative rotor incidence angles. Since no region of
low temperature drop corresponds clearly with a region of low local ef-
ficiency, it may be said that the stator blade wake regions cannot be
identified in these rotor-exit surveys.

3889

From the preceding considerations, the circumferential variation in angular momentum noted in figure 8 must result from effects of variations within the stator free stream. Expansion downstream of the stator throat. as required to obtain the design velocity diagrams appears to cause a circumferential variation in static pressure, which in turn results in a circumferential variation in the free-stream velocity and thus in angular momentum. The effect of a circumferential variation in static pressure in the free-stream regions of flow on the velocity distribution out of the stator for a constant total pressure is shown schematically in figure 9. The region of higher tangential velocity near the suction surface would result in the higher temperature drop across the turbine as compared with that of the regions of low tangential velocity near the pressure surface, provided both flow regions are turned to the same relative rotor-outlet flow angle. Even with subsonic flow through the stator, a circumferential variation in free-stream momentum may still be found if there is appreciable curvature in the streamlines downstream of the stator throat. The lower efficiency in the region of high temperature drop may be due to the effects of rotor incidence loss.

Actual Total-Pressure Loss

As previously discussed in BASIS FOR ANALYSIS, a total-pressure-loss parameter has been plotted for both turbines and is presented in figure 10. An inspection of these contours shows a large region of high total-pressure loss in the tip region for turbine 1 and in the mean-radius region for turbine 2. These trends are similar to those noted previously for the efficiency contours (fig. 3).

Circumferential variations in total-pressure loss are also evident from figure 10. Surveys made at the stator exit show that the total pressure in the free-stream regions is essentially uniform. Thus, any large radial variations in total-pressure loss in the regions of stator free-stream flow downstream of the rotor must be attributed to losses within the rotor. Downstream of the rotor the region of least total-pressure loss at a given radius is assumed to correspond to the regions of free-stream stator flow that is least affected by mixing effects of the stator losses. With this assumption, an indication of the radial variation in total-pressure loss caused by the rotor may be obtained by taking the difference between the minimum value of local total-pressure-loss parameter across the circumference at a given radius and the minimum value of total-pressure-loss parameter in the segment of the annulus and plotting this difference against radius for both turbines (fig. 11). The cross-hatched areas are arbitrarily called the end-wall regions. Figure 11 shows that a large region of high total-pressure loss occurs in the tip region of turbine 1, while a large region of high total-pressure loss occurs in the mean-radius region of turbine 2.

The difference in the position of the regions of high loss in the
two turbines is probably related to the blade surface upon which the high
diffusion and, therefore, the high loss takes place as well as the subse-
quent movements of these low-velocity fluids due to secondary flows. In
the case of turbine 1, large losses occur on the rear half of the rotor
suction surface where the radial pressure gradient due to radial equi-
librium is weak compared with the centrifugal-force field set up by the
rotation of the rotor. The low-velocity fluids are thus centrifuged
into the tip region to add to the losses originating there. In the case
of turbine 2, large losses take place over the first half of the rotor
pressure surface where the radial pressure gradient is strong compared
with the centrifugal-force field. As a result, large amounts of the low-
velocity fluids are moved towards the hub over the first portion of the
blade and toward the tip over the latter. Further, it is probable that
a considerable amount of these low-velocity fluids actually reaches the
hub of turbine 2 and is transported across the hub by the cross-channel
pressure gradient to the suction surface. Upon reaching the suction sur-
face, they accumulate until the centrifugal-force field becomes predomi-
nant and the low-velocity fluids are then centrifuged from the hub. It
appears that these fluids then leave the blade surface in the region of
the mean radius, thus causing large indicated loss in this region.

Secondary flows then cause a redistribution of the low-velocity
fluids on the rotor blade surfaces. This redistribution of the low-
velocity fluids affects mainly the local effective flow area and the
local effective surface contour. This means that the local loading on
the blade surface in the region of high loss may be very different from
that of design. The changes in local blade loading and local effective
flow area appear to be directly related to the radial variation in rotor-
exit angular momentum.

A small region of high total-pressure loss is noted in the tip re-
gion of turbine 2 (fig. 11(b)). This region is probably caused by the
effects of rotor-tip cross-channel secondary flows. No region of total-
pressure loss is distinguishable as being the effect of tip secondary
flows for turbine 1 (fig. 11(a)). The quantity of low-velocity fluids
flowing into this region for this turbine is so large that any tip sec-
ondary flow losses are probably obscured. In the region near the hub
of turbine 1 a small region of loss is evident. This region can also be
attributed to an accumulation of loss due to hub secondary flows. For
turbine 2, however, no such accumulation is evident. This difference
can be attributed to the transport of low-velocity fluids from the hub
region into the region of high loss at the mean by centrifugal force.

By applying the radial variations in loss given in figure 11 to the
respective contours in figure 10, new contours of total-pressure-loss
parameter were obtained, which are presented in figure 12. This was ac-
complished by adding the loss at a given radius for a given turbine

(fig. 11) to every circumferential position at that radius (fig. 10). These figures indicate the variation in losses in total pressure coming into the rotor. Since these contours are not directly comparable with the contours of total-pressure ratio made at the exit of the stator, it is evident that considerable mixing and distortion of the stator flow pattern have taken place. Comparison of figure 12 with a stator survey (fig. 13) taken in the same axial plane as these rotor-exit surveys but with the rotor removed (ref. 3) indicates a similarity in the tip region. No similarity, however, can be seen between the other regions of figures 12 and 13. The circumferential variations in the hub and mean regions of the corrected total-pressure-loss contours are probably due to the effects of circumferential variations in the regions of stator free-stream flow.

CONCLUDING REMARKS

The results of this investigation show that a description of the flow characteristics through a single-stage turbine can be obtained from the survey results taken at the rotor exit. Furthermore, some of the major factors that influence the measured flow patterns may be qualitatively isolated, thus facilitating their analysis.

The survey results of two similar transonic turbines, but with relatively high diffusion on different surfaces of the rotor blades, indicate that considerable circumferential variations in momentum existed at the stator exit that are attributable to variations in the regions of stator free-stream flow. At the rotor exit large radial variations in angular momentum and total-pressure loss were found.

The radial variations of total-pressure loss and rotor-outlet angular momentum for the two turbines differed because of (1) the blade surface upon which the high diffusion and therefore the high loss occurred, and (2) the subsequent secondary-flow path which the low-velocity fluids followed through the rotor.

Premature choking of the rotor of the high-suction-surface-diffusion turbine was indicated by higher-than-design rotor-outlet angular momentum at design work output. A slight mismatch between the stator and rotor throat areas of the high-pressure-surface-diffusion turbine was indicated at design work output by lower-than-design rotor-outlet angular momentum.

Lewis Flight Propulsion Laboratory
    National Advisory Committee for Aeronautics
        Cleveland, Ohio, November 28, 1955

3889

CI-2

APPENDIX A

SYMBOLS

c_p specific heat at constant pressure

g acceleration due to gravity, 32.17 ft/sec^2

J mechanical equivalent of heat, 778 ft-lb/Btu

L total-pressure-loss parameter $= 1 - \dfrac{P'_o}{P'_i} \left(\dfrac{T'_i}{T'_o}\right)^{\frac{\gamma}{\gamma-1}}$

P absolute pressure, lb/sq ft

$\bar{P}$ average absolute pressure at a given radius, lb/sq ft

r radius, ft

T absolute temperature, $^\circ$R

V absolute velocity, ft/sec

$\bar{V}$ average absolute velocity at given radius, ft/sec

W relative velocity

$\bar{\alpha}$ average absolute rotor-outlet flow angle measured from axial direction, deg

γ ratio of specific heats

η_l local adiabatic efficiency based on measured values of inlet and outlet total-state measurements

ω angular velocity, radians/sec

Subscripts:

cr   condition at Mach number of 1.0

d   design values

i   turbine-inlet

o   turbine-outlet

M   measured values

t   tip

test   test conditions

u   tangential direction

z   axial direction

Superscripts:

'   total state

"   relative total state

APPENDIX B

METHOD OF COMPUTING ROTOR-EXIT ANGULAR-MOMENTUM PARAMETER

The radial variation in rotor-exit angular-momentum parameter $\omega r \overline{V}_{u,M}/gJc_p T_i'$ was calculated as follows:

An average measured value of tangential velocity $\overline{V}_{u,M}$ was calculated from mean values of measured local total-pressure and outlet flow angles at the rotor exit and from assuming a linear variation between the static pressure measured at the hub and tip. These mean values were obtained by arithmetically averaging the total-pressure and angle readings along the circumference at a given radius. The static pressure at a given radius was obtained by assuming that a linear variation exists between the static pressures measured at the hub and the tip. From the static pressure and average value of total pressure at a given radius, an average velocity was computed in terms of a ratio $\overline{V}/V_{cr}$ from

$$\frac{P}{P'} = \left[1 - \frac{\gamma - 1}{\gamma + 1} \left(\frac{\overline{V}}{V_{cr}} \right)^2 \right]^{\frac{\gamma}{\gamma - 1}}$$

The critical velocity V_{cr} was found from the average rotor-outlet total temperature as obtained from torque, speed, weight-flow measurements, and inlet total temperature. This temperature was used instead of the measured local values, because the use of the measured local values was found to have a very small effect on the final result. From the average velocity computed for each radial position, the tangential component was computed from

$$\overline{V}_{u,M} = \overline{V} \sin \overline{\alpha}_o$$

using the mean value of measured outlet flow angle.

The design tangential velocities at test conditions were obtained by taking the design values and correcting them to test conditions by

$$V_{u,d,test} = V_{u,d} \frac{V_{cr,i,test}}{V_{cr,i,d}}$$

REFERENCES

1. Wong, Robert Y., Monroe, Daniel E., and Wintucky, William T.: Investigation of Effect of Increased Diffusion of Rotor-Blade Suction-Surface Velocity on Performance of Transonic Turbine. NACA RM E54F03, 1954.

2. Miser, James W., Stewart, Warner L., and Monroe, Daniel E.: Effect of High Rotor Pressure-Surface Diffusion on Performance of a Transonic Turbine. NACA RM E55H29a, 1955.

3. Stewart, Warner L.: Investigation of Compressible Flow Mixing Losses Obtained Downstream of a Blade Row. NACA RM E54I20, 1954.
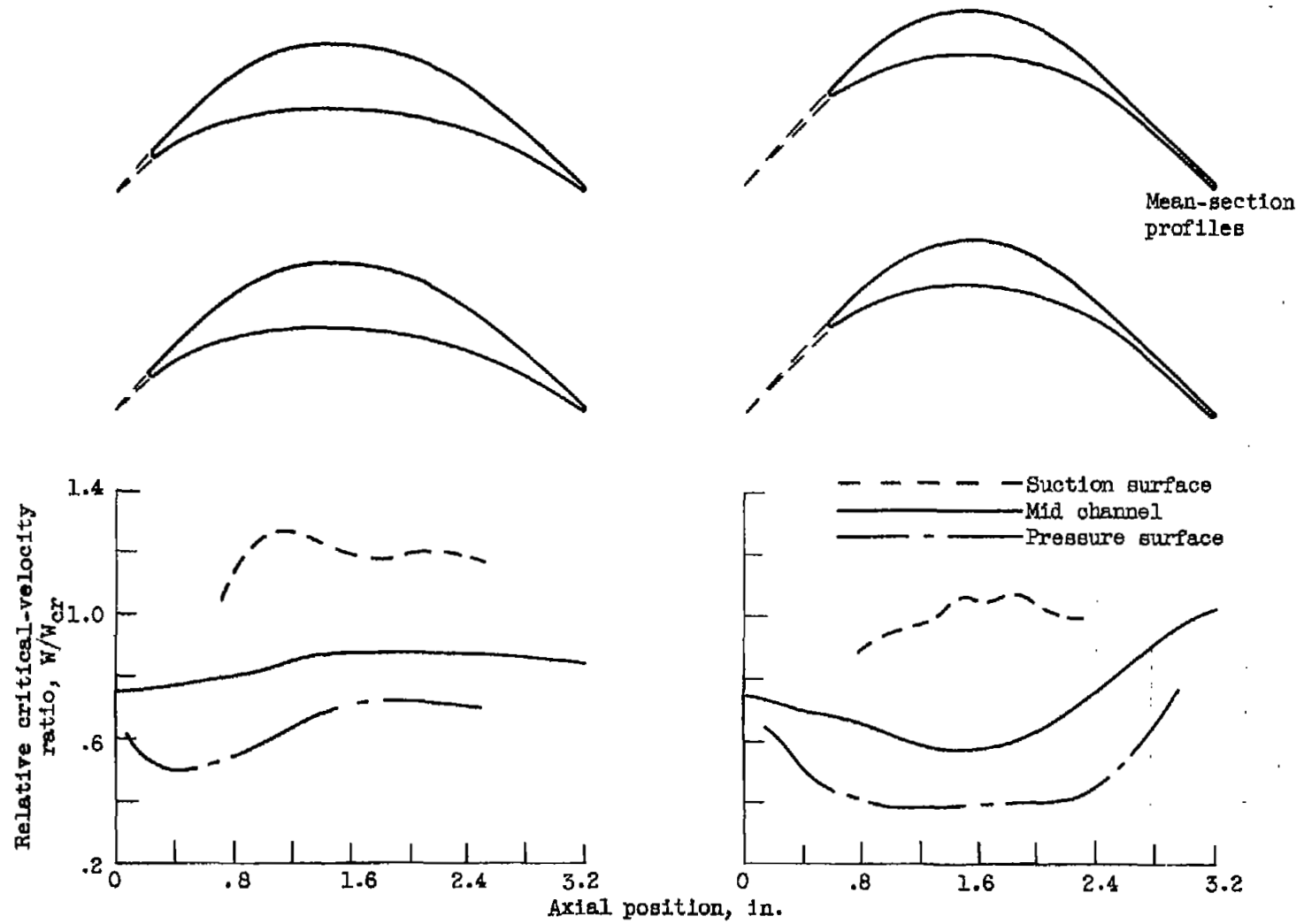
3889

Figure 1. - Rotor mean-section profiles and design velocity distributions.

3889

Stator blades

Flow

Total-pressure
variation rela-
tive to stator

Rotor blades

Direction of
rotation

Flow relative
to rotor

Total-pressure
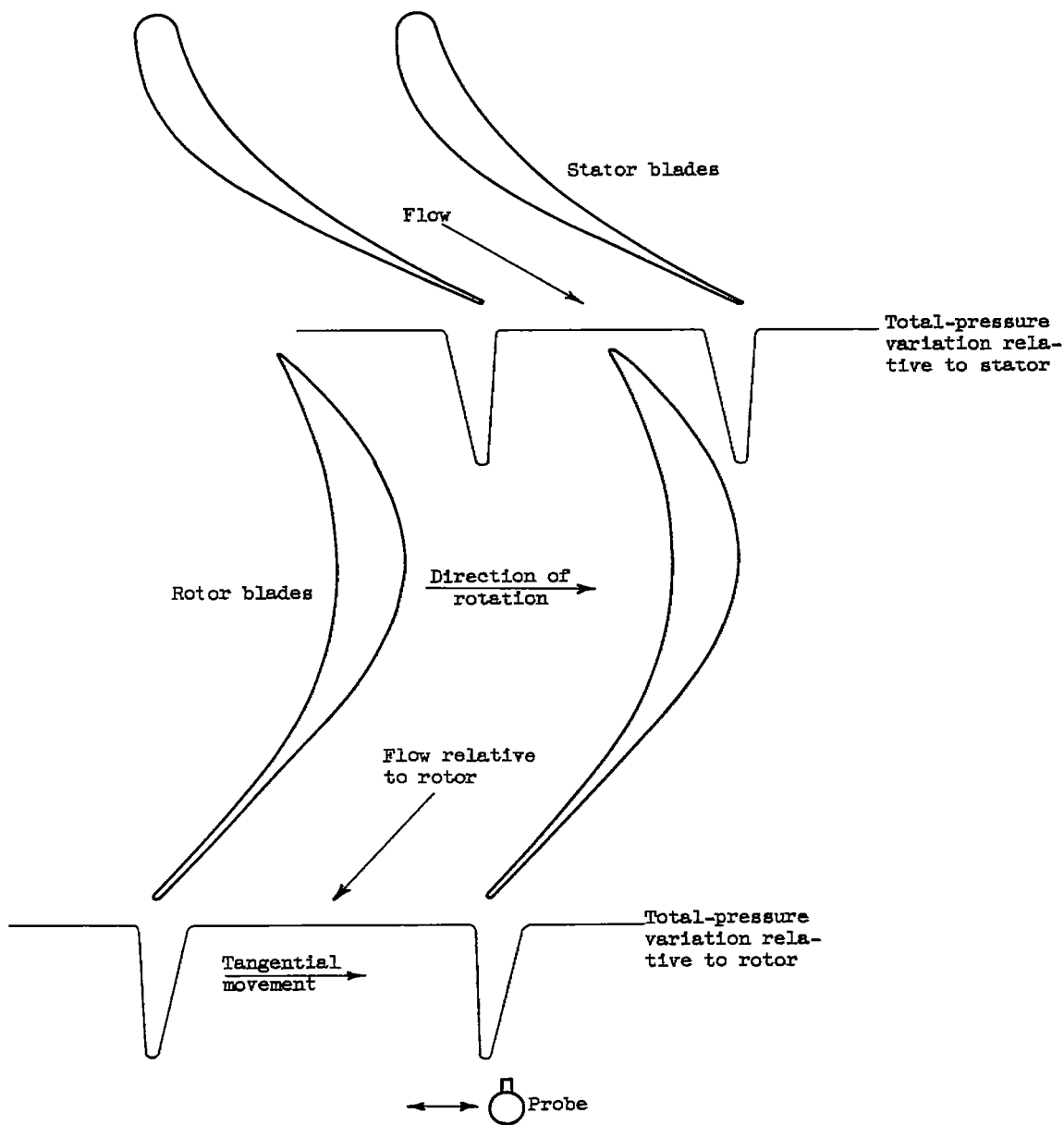variation rela-
tive to rotor

Tangential
movement

Probe

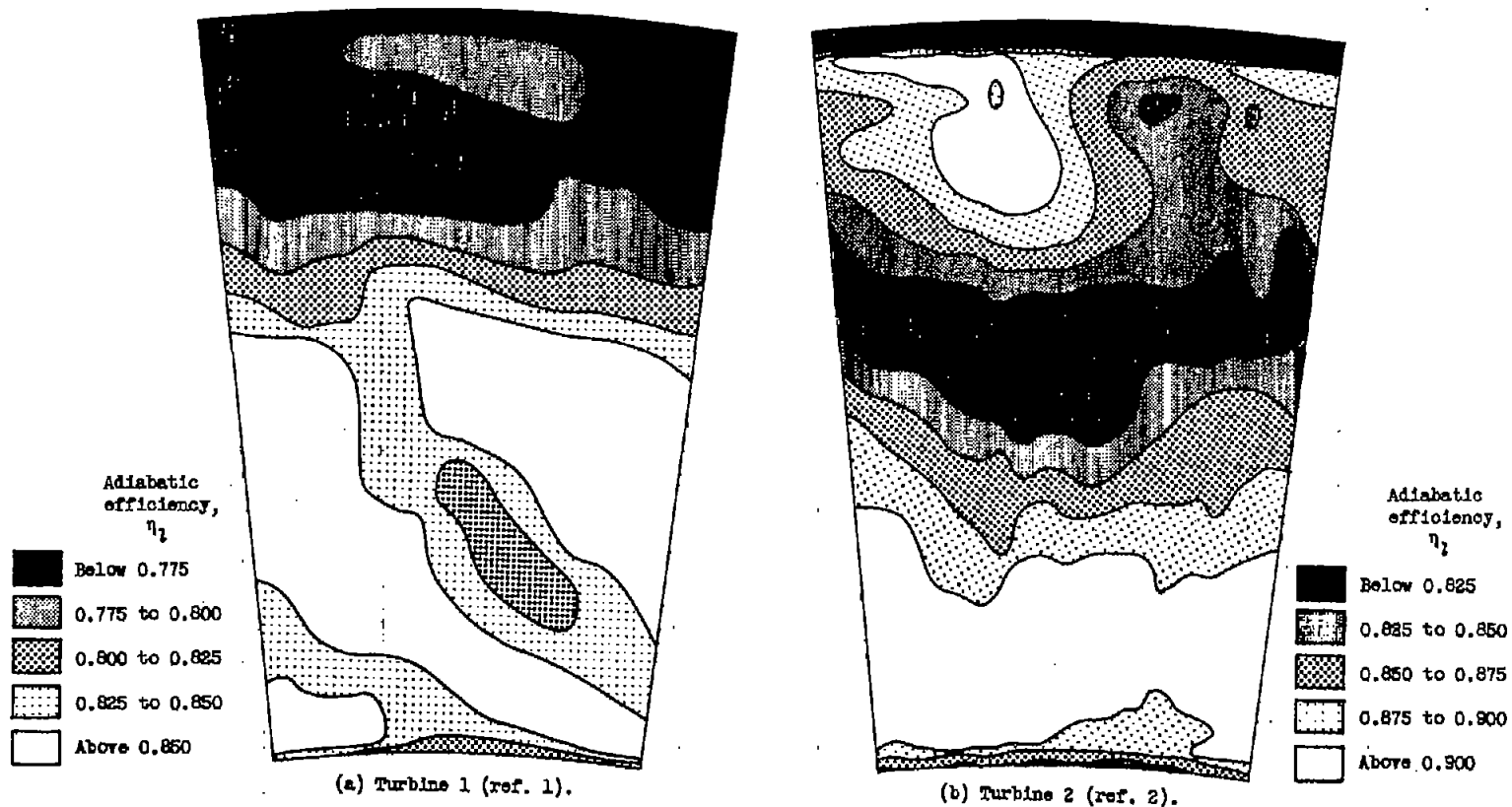Figure 2. - Schematic diagram of circumferential total-pressure
variations in single-stage turbine.

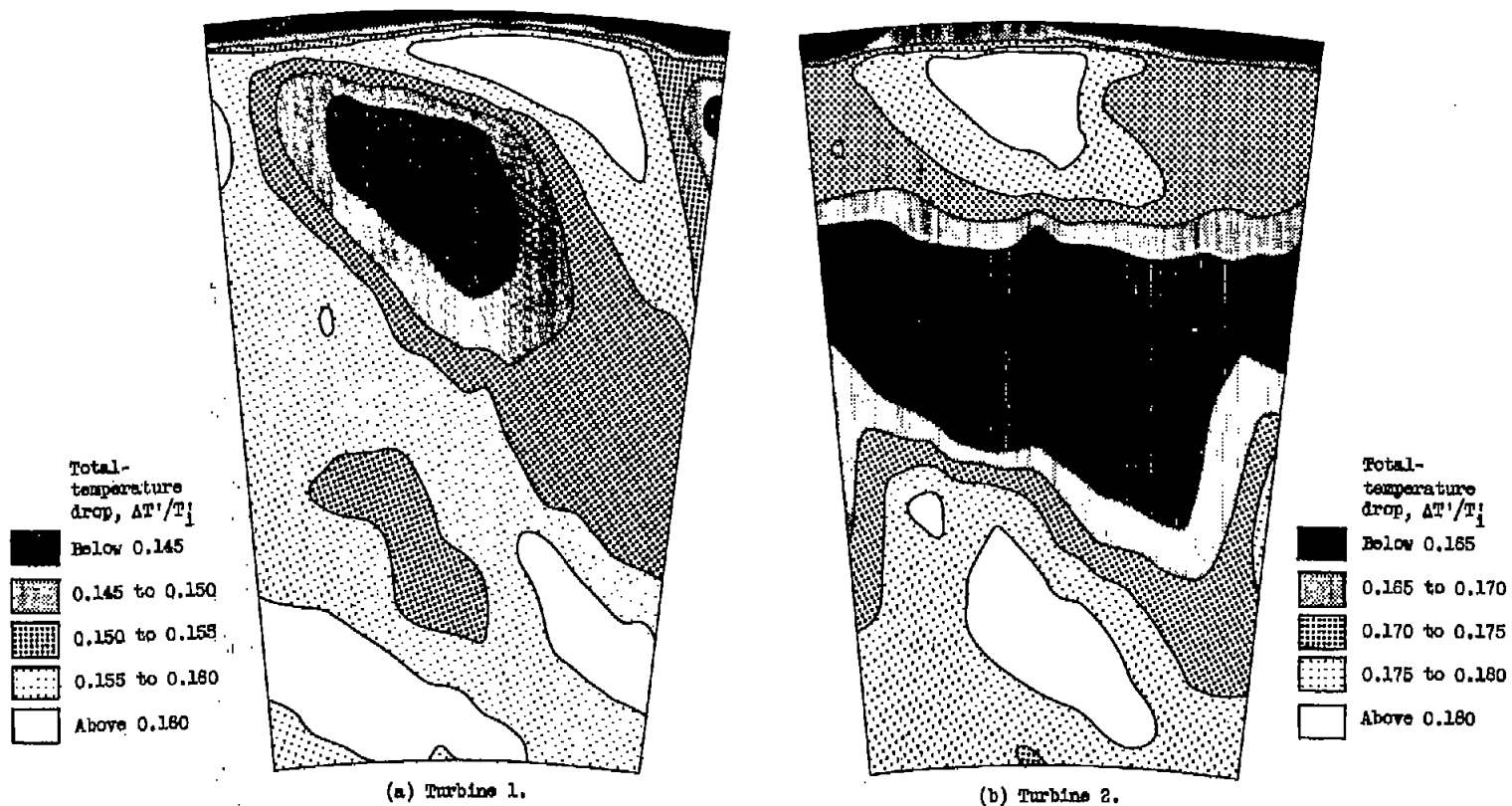Figure 3. - Contours of constant local adiabatic efficiency.

(a) Turbine 1 (ref. 1).

(b) Turbine 2 (ref. 2).

Adiabatic
efficiency,
η_i

Below 0.775

0.775 to 0.800

0.800 to 0.825

0.825 to 0.850

Above 0.850

Adiabatic
efficiency,
η_i

Below 0.825

0.825 to 0.850

0.850 to 0.875

0.875 to 0.900

Above 0.900

(a) Turbine 1.

(b) Turbine 2.

Figure 4. - Contours of constant total-temperature drop.

Total-
pressure
drop,
$\Delta P'/P_i'$

Above 0.56

0.54 to 0.56

0.52 to 0.54

0.50 to 0.52

Below 0.50

(a) Turbine 1.

(b) Turbine 2.

Figure 5. - Contours of constant local total-pressure drop.

5889

CI-3 back
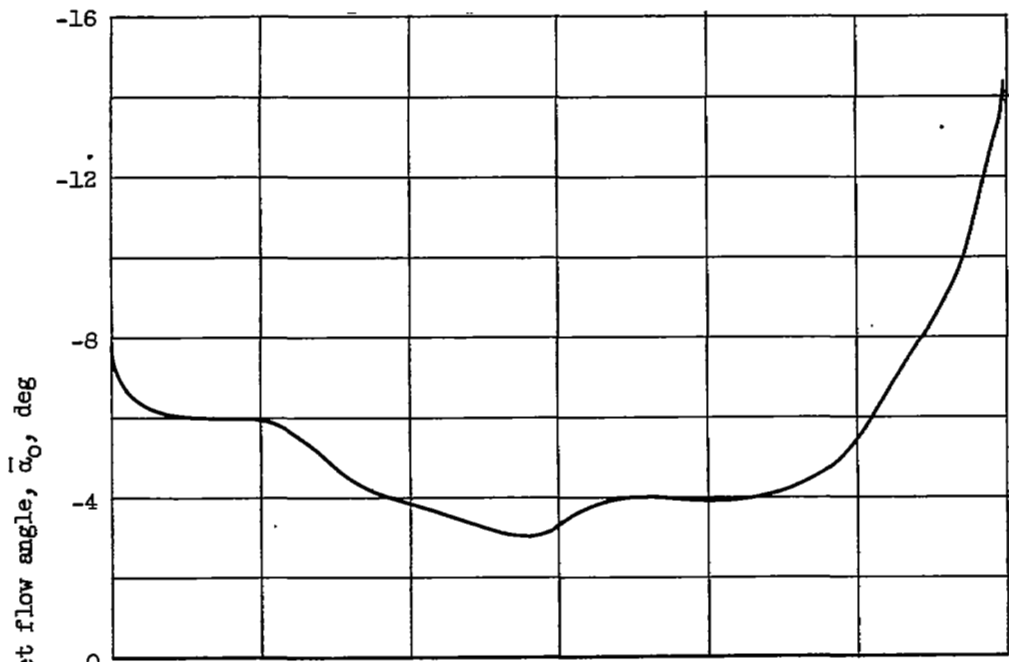
(a) Turbine 1.
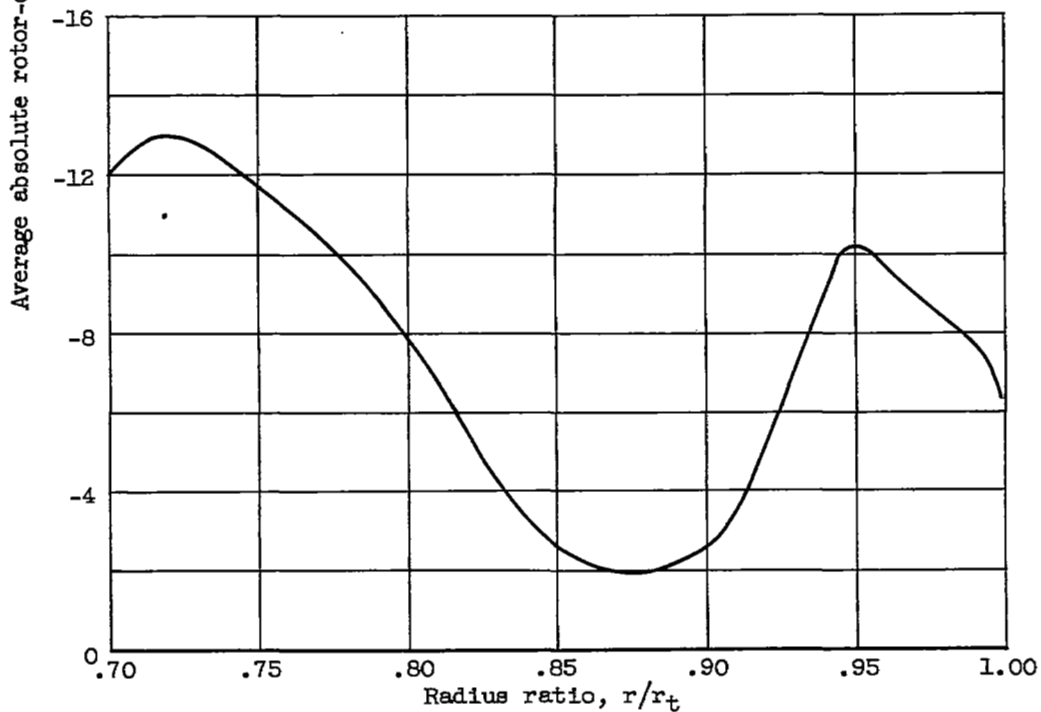
(b) Turbine 2.

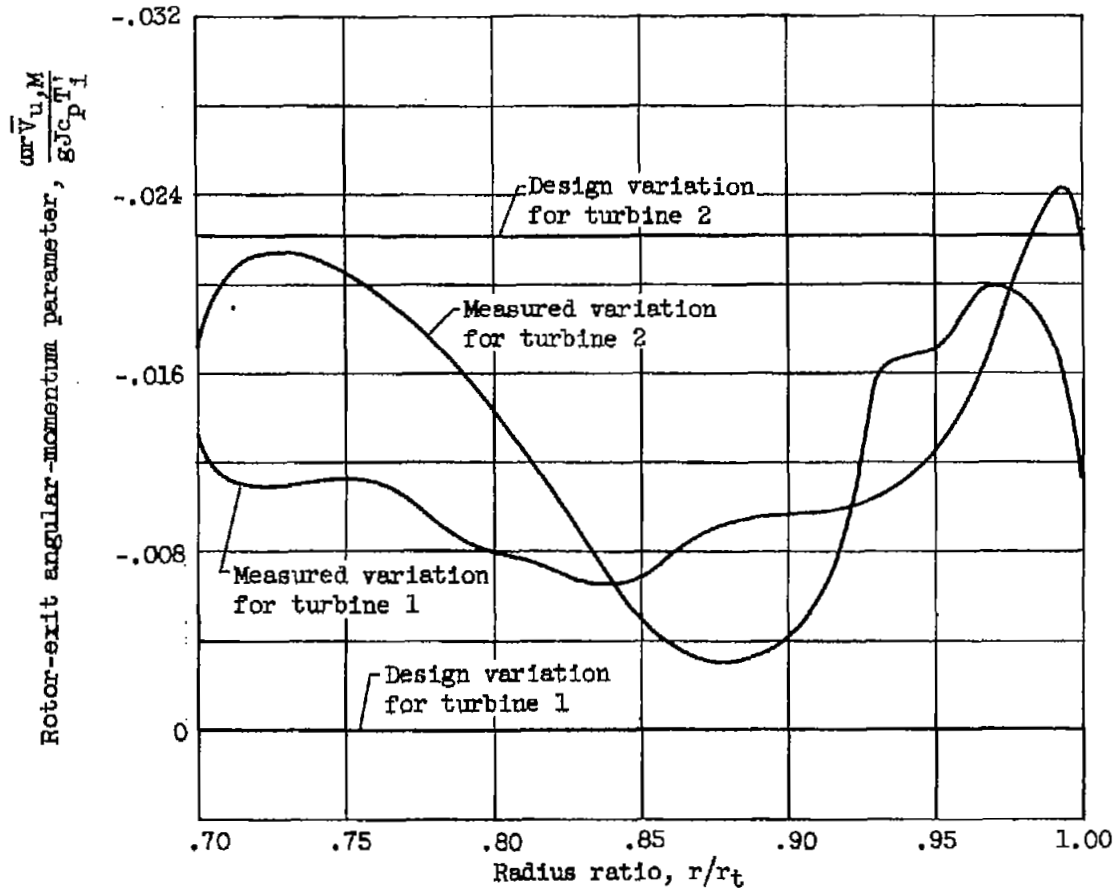Figure 6. - Radial variation in absolute rotor-outlet flow angle.

Figure 7. - Radial variation in rotor-exit angular momentum.

Angular-
momentum
parameter,
$\dfrac{\alpha r V_u}{g J c_p T_1'}$

Below 0.135

0.135 to 0.140

0.140 to 0.145

0.145 to 0.150

Above 0.150

Angular-
momentum
parameter,
$\dfrac{\alpha r V_u}{g J c_p T_1'}$

Below 0.150

0.150 to 0.155

0.155 to 0.160

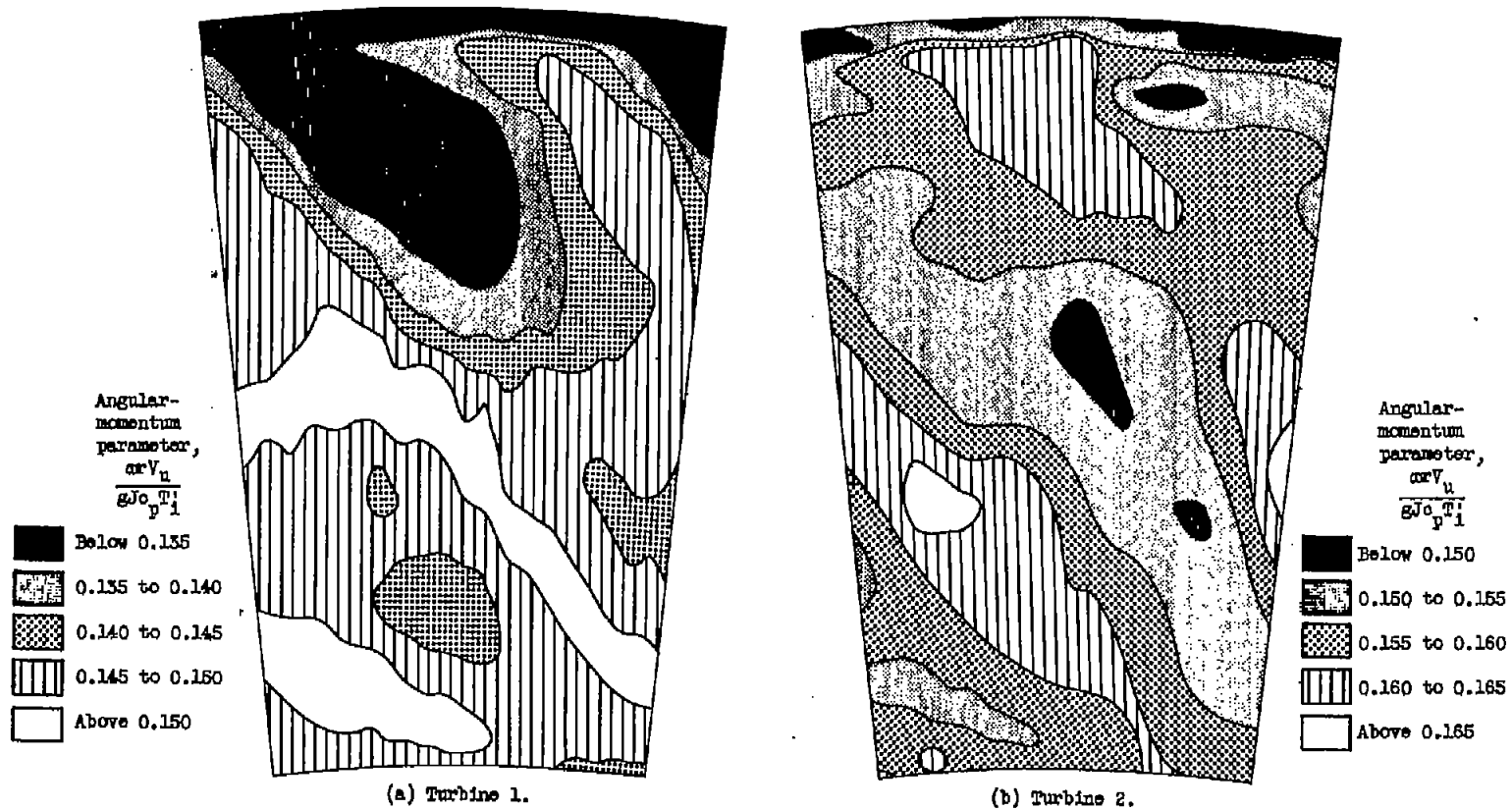0.160 to 0.165

Above 0.165

(a) Turbine 1.

(b) Turbine 2.

Figure 8. - Contours of constant rotor-inlet angular momentum.
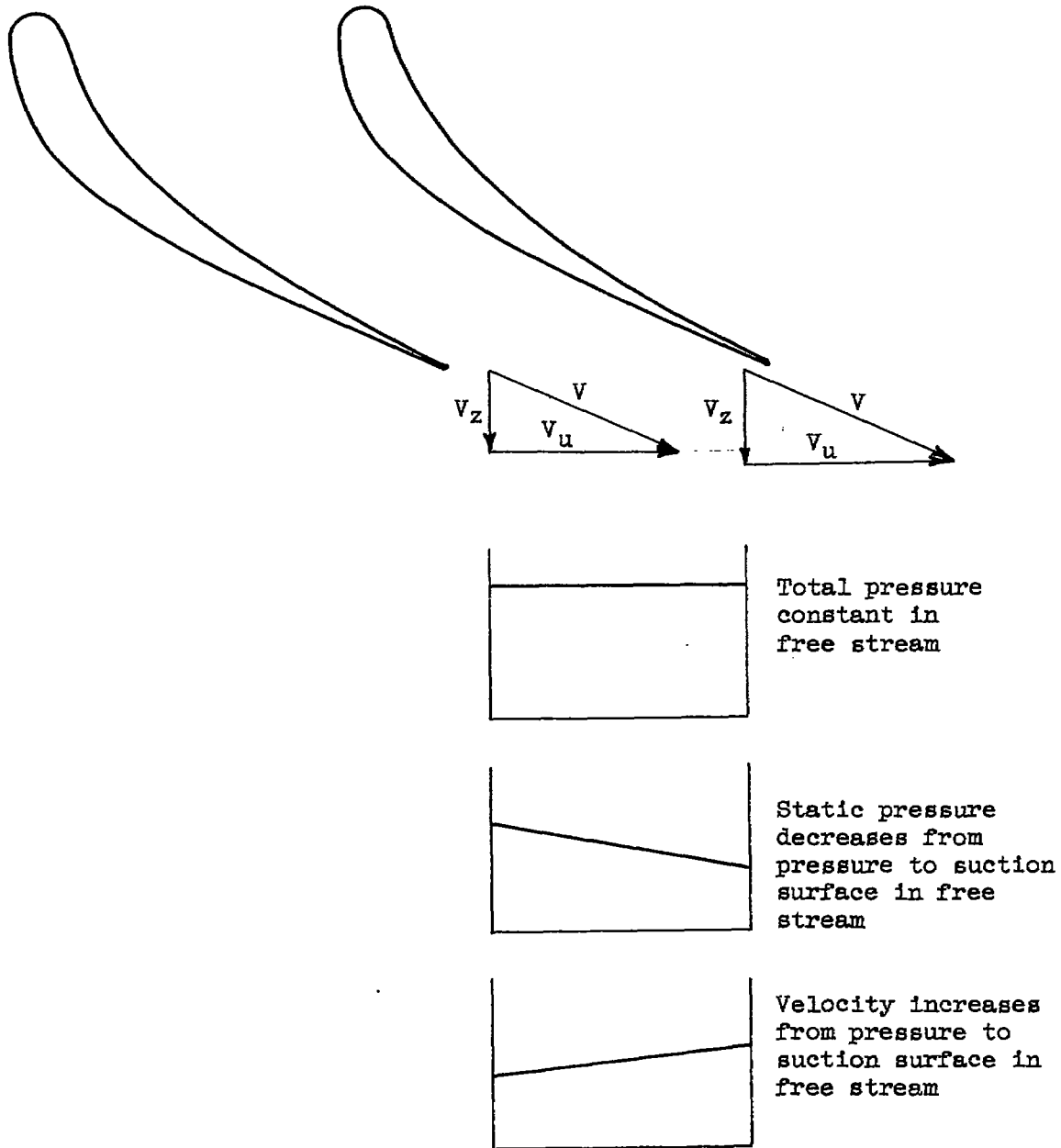
Figure 9. - Schematic diagram of variation of total pressure, static pressure, and velocity in free-stream flow at stator exit.
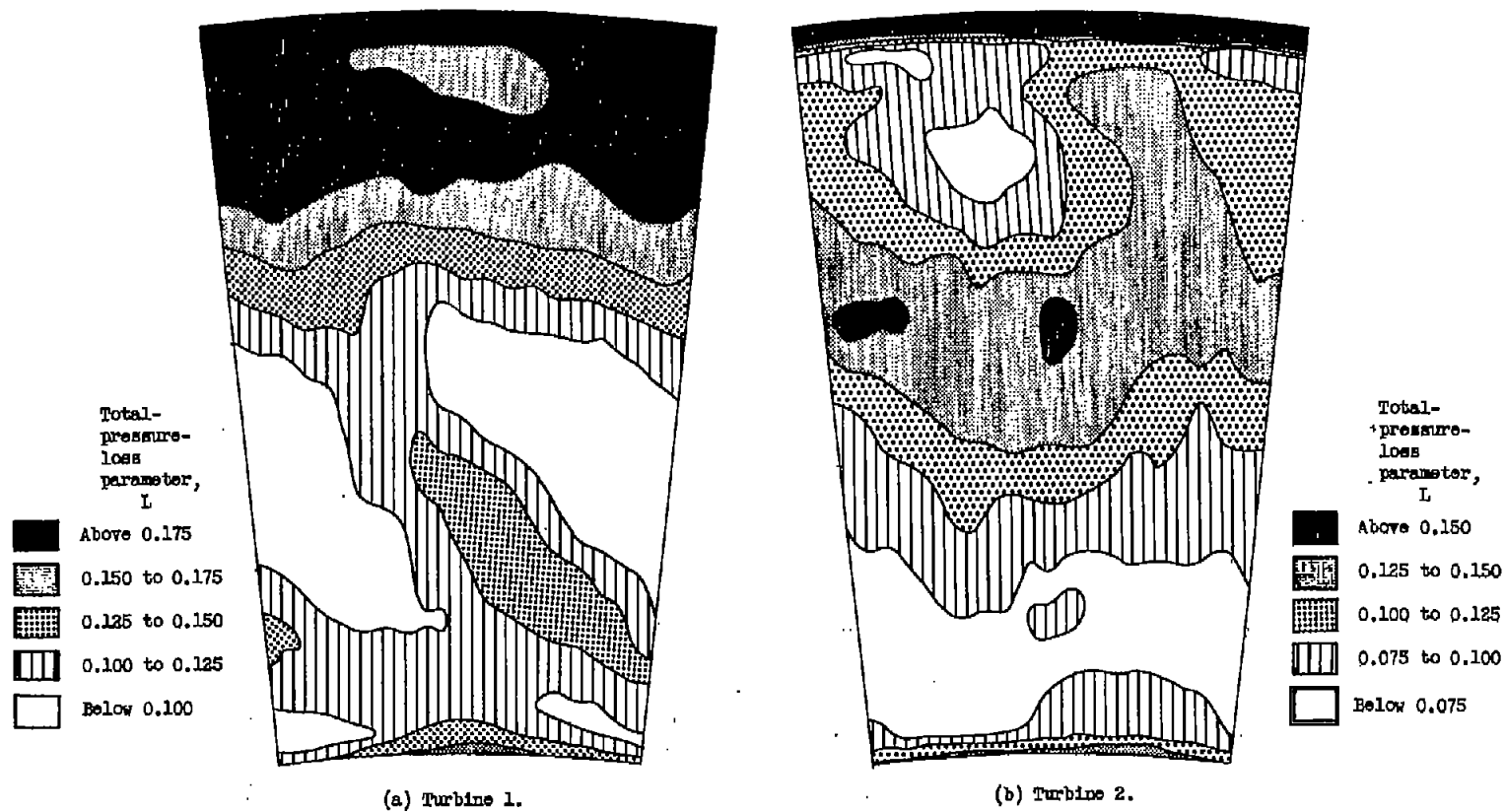
Total-
pressure-
loss
parameter,
L

Above 0.175

0.150 to 0.175

0.125 to 0.150

0.100 to 0.125

Below 0.100

Total-
pressure-
loss
parameter,
L

Above 0.150

0.125 to 0.150

0.100 to 0.125

0.075 to 0.100

Below 0.075

(a) Turbine 1.

(b) Turbine 2.

Figure 10. - Contours of constant local total-pressure-loss parameter.

(a) Turbine 1.

(b) Turbine 2.
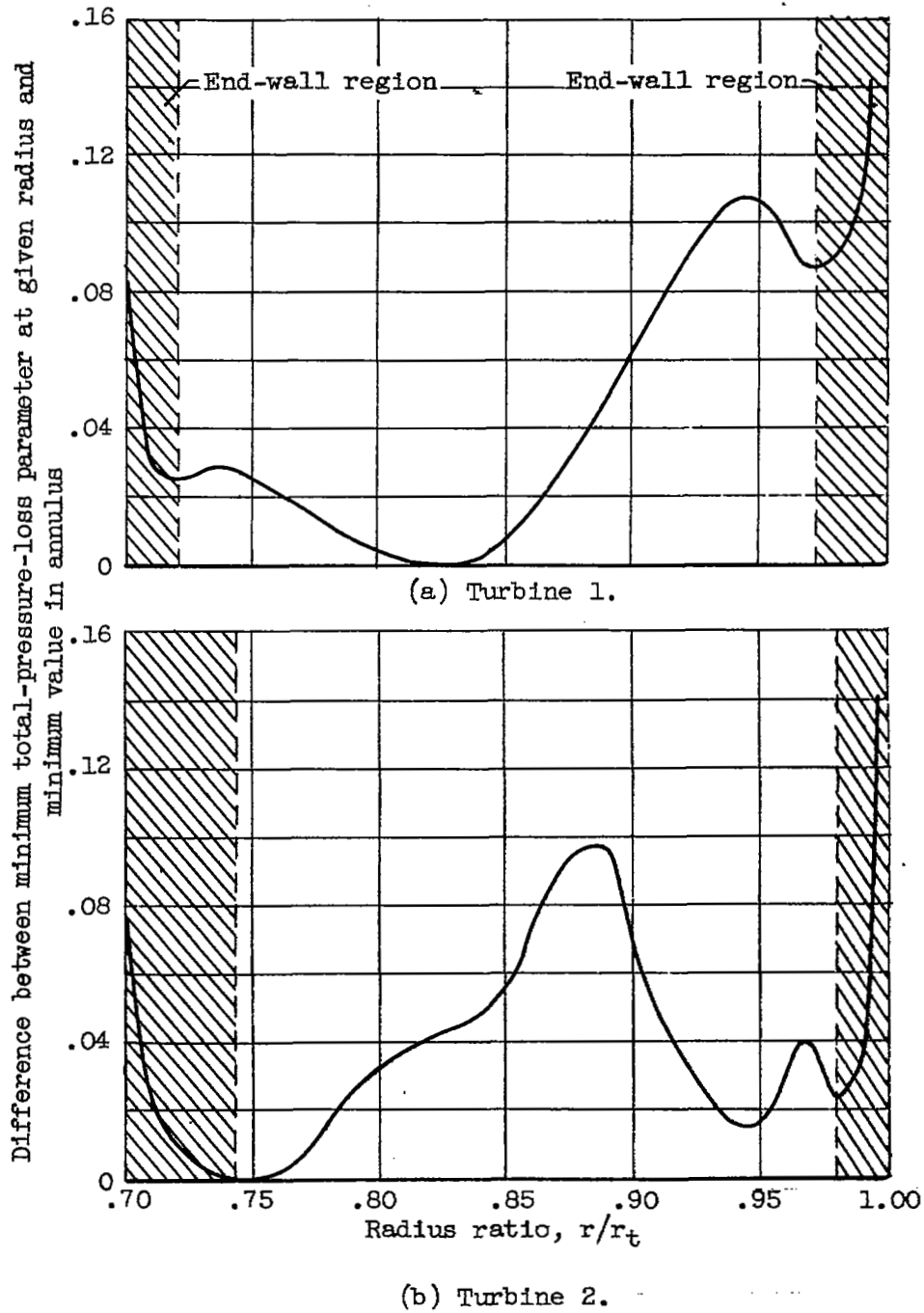
Figure 11. - Radial variation in total-pressure
loss that is attributable to rotor effects.

Total-
pressure-
loss
parameter,
L

■ Above 0.150

▒ 0.125 to 0.150

▒ 0.100 to 0.125

▨ 0.075 to 0.100

☐ Below 0.075

Total-
pressure-
loss
parameter,
L

■ Above 0.125

▒ 0.100 to 0.125

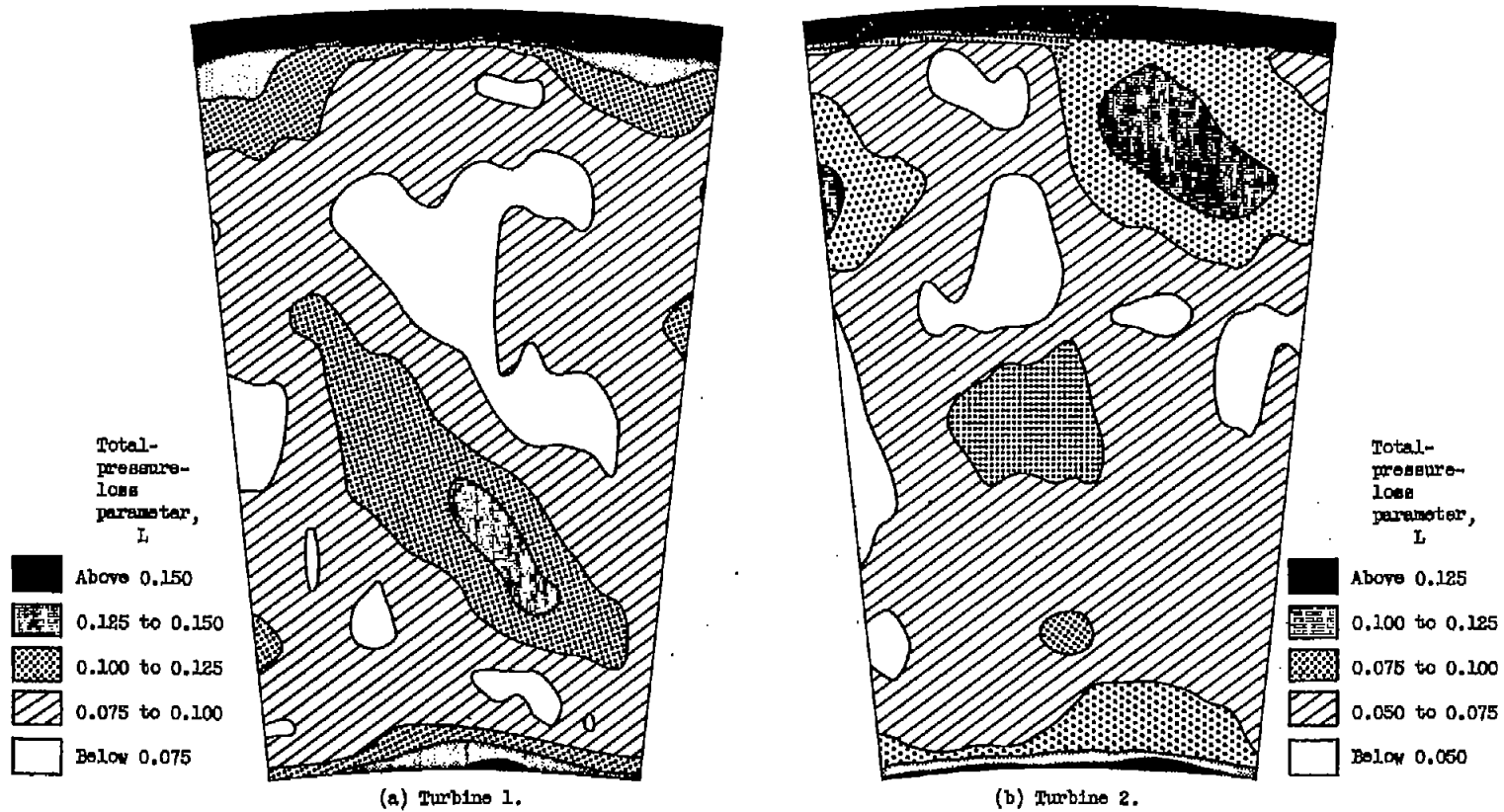▒ 0.075 to 0.100

▨ 0.050 to 0.075

☐ Below 0.050

(a) Turbine 1.

(b) Turbine 2.

Figure 12. - Contours of constant local total-pressure-loss parameter adjusted
to remove radial variation in rotor-induced losses.

Total-pressure
ratio, P_o'/P_i'

☐ Above 0.96

▦ 0.95 to 0.96

▦ 0.94 to 0.95

▨ 0.92 to 0.94

▨ 0.90 to 0.92

■ Below 0.90
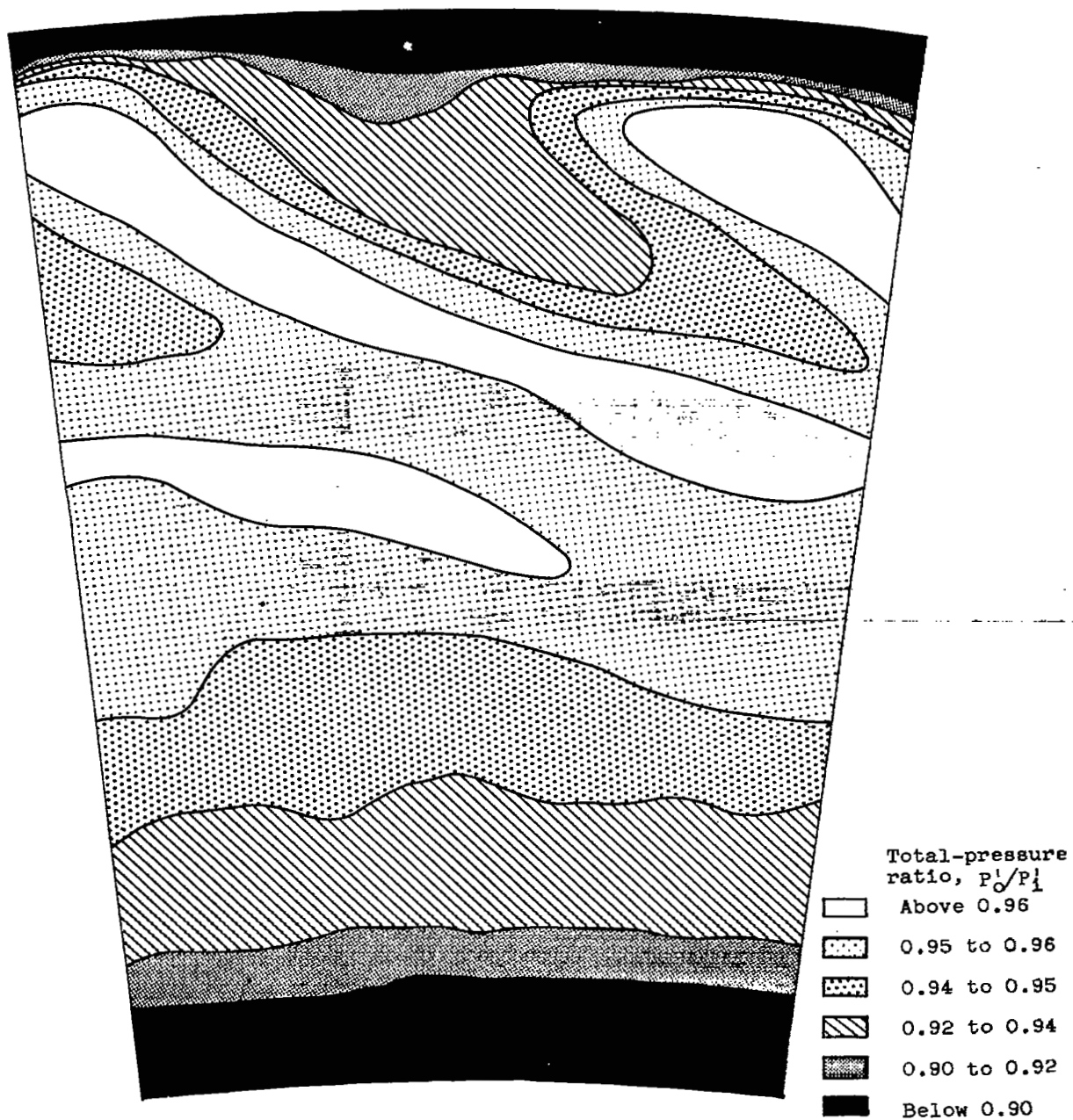
Figure 13. - Results of stator total-pressure survey made
    in plane of rotor-exit survey.